QCD equation of state and cosmological parameters in the early universe

P. Castorina,[1,2] V. Greco,[1,3] and S. Plumari[1,3]

[1]*Dipartimento di Fisica e Astronomia, Università di Catania, Via Santa Sofia, 64, 95123 Catania, Italy*
[2]*INFN Sezione di Catania, Via Santa Sofia 64, I-95123 Catania, Italy*
[3]*INFN Laboratori Nazionali del Sud, Via Santa Sofia 62, I-95123 Catania, Italy*

(Received 21 July 2015; published 22 September 2015)

The time evolution of cosmological parameters in the early Universe at the deconfinement transition is studied by an equation of state (EoS) which takes into account the finite baryon density and the background magnetic field. The nonperturbative dynamics is described by the field correlator method which gives, with a small number of free parameters, a good fit of lattice data. The entire system has two components, i.e., the quark-gluon plasma and the electroweak sector, and the solutions of the Friedmann equation show that the scale factors $a(t)$ and $H(t) = (1/a)da/dt$ are weakly dependent on the EoS, but the deceleration parameter $q(t)$ and the jerk $j(t)$ are strongly modified above the critical temperature T_c, corresponding to a critical time $t_c \simeq 20$–25 μs. The time evolution of the cosmological parameters suggests that above and around T_c, there is a transient state of acceleration typical of a matter-dominated universe; this is entailed by the QCD strong interaction. The effect of the hadronic matter below T_c does not qualitatively change the previous behavior and one can consistently follow the cosmological evolution up to 100 μs.

DOI: 10.1103/PhysRevD.92.063530 PACS numbers: 25.75.-q, 25.75.Dw, 25.75.Nq

I. INTRODUCTION

Lattice simulations of quantum chromodynamics (QCD) and phenomenological analyses of relativistic heavy ion collisions data clearly indicate that the transition from a quark-gluon plasma to colorless states occurs in a nonperturbative regime. For vanishing chemical potential, μ_B, lattice QCD simulations show that it is a cross-over at a (pseudo) critical temperature $T_c \simeq 154 \pm 9$ Mev [1–4] while for large μ_B several effective field theories suggest that the transition is of first order [5–8]. The use of the appropriate QCD equation of state including the phase transition to hadronic matter is important for the phenomenology of heavy-ion collision experiments. In particular, it has been shown that it affects the expansion of the quark gluon plasma and it is crucial for the correct description of the Hanbury-Brown-Twiss radii [9,10].

Moreover, lattice QCD in a background magnetic field B shows [11,12] that the transition temperature is reduced by the magnetic field.

The previous parameters T, μ_B and B give different and important information on the dynamics of the phase transition which, in turn, has strong implications at the cosmological level in the early Universe (see [13–16] for a recent review). In particular, the equation of state (EoS) in the quark-gluon plasma phase affects directly the density fluctuations of the thermodynamic quantities [17–20] and the emission of gravitational waves [17,21–25] during the cosmological evolution.

In Ref. [17] the density fluctuations in the early Universe have been studied by using the MIT bag model EoS and the old lattice QCD EoS with a first-order deconfinement phase transition. A more recent and realistic QCD EoS has been introduced in Ref. [19] improving the reliability of the calculations of the fluctuations and of the modifications in the time evolution of the cosmological scale factor $a(t)$. The effects of the external magnetic field on the energy density fluctuations have been considered in Ref. [18] by a phenomenological QCD EoS which includes B. An analogous analysis for finite density with different variants of the MIT bag model has been carried out in Ref. [20].

The results of the previous studies show a smooth time dependence of the thermodynamic quantities; however, they essentially consider the effect of the transition on the thermodynamic fluctuations and on the scale factor.

In this paper we shall analyze the modifications on the early Universe's evolution by using a realistic EoS which depends on T, μ_B and B, with a particular focus on the evolution of the cosmological parameters rather than on the fluctuations.

To describe the EoS in the quark-gluon plasma phase, we shall apply the field correlator method (FCM) [26]. This specific choice is motivated by the nonperturbative dynamics of the FCM which describes, with a small number of free parameters, lattice data of the thermodynamics quantities (pressure and energy density) at finite temperature and their dependence on μ_B and B [27–29]. Here we will also show that its extension to a finite B [30,31] captures correctly the main features of lQCD EoS under a magnetic field.

The discussion of the combined effects of the chemical potential and of the external magnetic field, during the deconfinement transition, in the Friedmann equations is of interest in its own right. However, as we shall see, the most interesting results are on the behavior of the deceleration

parameters q and the jerk j, defined as ($'$ indicates the time derivative)

$$q = -\frac{a''a}{a'^2} \tag{1}$$

$$j = \frac{a'''a^2}{a'^3}, \tag{2}$$

which have an important role in describing the cosmological evolution [32,33].

Indeed, it turns out that the deceleration and the jerk are strongly modified above the critical temperature T_c, corresponding to a critical time $t_c \simeq 20$–25 μs, and that the EoS and the time evolution of the cosmological parameters suggest that above and near T_c, the system has the typical behavior of a matter-dominated universe, with clusters of colored particles, which evolves towards a radiation-dominated universe. The introduction of the hadronic degrees of freedom, by a hadron resonance gas, below T_c does not qualitatively change this conclusion.

The plan of the paper is as follows. In Sec. I we shall consider the relevant cosmological equations and parameters. The FCM, with the dependence on μ_B and B, is recalled and compared with lattice data in Sec. II. Section III is devoted to the solution of the Friedmann equation with the FCM EoS, and Sec. IV contains the electroweak contributions to the EoS of the entire dynamical system. In Sec. V the results on the cosmological parameters are discussed, and our comments and conclusions are in Sec. VI.

II. COSMOLOGICAL PARAMETERS

The parameters $H(t) = a'/a$, $q(t)$ and $j(t)$ can naturally be defined making use of a Taylor series for the scale factor $a(t)$ near a generic time t^*,

$$a(t) = a(t^*) + a'(t^*)(t-t^*) + \frac{1}{2}a''(t^*)(t-t^*)^2 + \frac{1}{3!}a'''(t^*)(t-t^*)^3 + \cdots, \tag{3}$$

which can be written as

$$a(t) = a(t^*)[1 + H(t^*)(t-t^*) - \frac{1}{2}(qH^2)(t^*)(t-t^*)^2 + \frac{1}{3!}(jH^3)(t^*)(t-t^*)^3 + \cdots. \tag{4}$$

Basic characteristics of the cosmological evolution, both static and dynamical, can be expressed in terms of H_0, the present time value of $H(t)$, and the deceleration q_0. The other parameters, i.e., the higher time derivatives of the scale factor, enable us to construct the model-independent kinematics of the cosmological expansion.

Indeed, cosmological models can be tested by expressing the Friedmann equation in terms of directly measurable cosmological scalars constructed out of higher derivatives of the scale factor, i.e., $q, j, \ldots$ [32,33].

To illustrate this aspect, let us consider a simple two-component universe filled with nonrelativistic matter with density M_m/a^3 and radiation with density M_r/a^4 (M_m, M_r constants) which do not interact with each other [33] and are without a magnetic background. By writing the Friedmann equation in the form ($8\pi G/3 = 1$)

$$\frac{a'^2}{a^2} + \frac{k}{a^2} = \frac{M_m}{a^3} + \frac{M_r}{a^4} \tag{5}$$

and differentiating twice with respect to t, one gets

$$a'' = -\frac{1}{2}\frac{M_m}{a^2} - \frac{M_r}{a^3} \tag{6}$$

and

$$a''' = \frac{M_m}{a^3}a' + 3\frac{M_r}{a^4}a'. \tag{7}$$

Then the deceleration and the jerk can be written as $q = A/2 + R$ and $j = A + 3R$, where $A = M_m/a^3H^2$ and $R = M_r/a^4H^2$. For a flat universe filled only with nonrelativistic matter, one has $R = 0$, $q = 1/2$, $A = 1$, and $j = 1$; if one considers only radiation, then $A = 0$, $q = 1$, $R = 1$, and $j = 3$. A deviation from these values of q and j indicates a mixture of matter and radiation and/or an interaction between the two components. Indeed, the same values can be easily obtained by a simple application of the Friedmann equation (for $k = 0$), written as

$$\frac{a'}{a} = -\frac{d\epsilon/dt}{3(\epsilon + p)} = \sqrt{\frac{8\pi G}{3}}\sqrt{\epsilon}, \tag{8}$$

by the EoS $p = c_s^2\epsilon$ with a constant speed of sound. The analytic solution is

$$\epsilon(t) = \frac{4\epsilon(t_0)}{\left[3\sqrt{\frac{8\pi G\epsilon(t_0)}{3}}(1+c_s^2)(t-t_0) + 2\right]^2} \tag{9}$$

and

$$\frac{a(t)}{a(t_0)} = \left[\frac{3}{2}\sqrt{\frac{8\pi G\epsilon(t_0)}{3}}(1+c_s^2)(t-t_0) + 1\right]^{\frac{2}{3(1+c_s^2)}} \tag{10}$$

and one obtains

$$q = -\frac{a''a}{a'^2} = \frac{1+3c_s^2}{2} \tag{11}$$

$$j = \frac{a''' a^2}{a'^3} = \left(\frac{1+3c_s^2}{2}\right)(2+3c_s^2) \tag{12}$$

which reproduce the previous values for a matter-dominated ($c_s^2 = 0$) and radiation-dominated ($c_s^2 = 1/3$) universe.

In general, the speed of sound is not constant, and in the next sections we shall discuss the behavior of the cosmological parameters q and j during the deconfinement transition on the basis of the Friedmann equation (8) and by using the energy density ϵ and the pressure p in the FCM, after fitting the QCD lattice data at finite temperature μ_B and B.

III. FIELD CORRELATOR METHOD

Many phenomenological models of QCD at finite temperature and density cannot make reliable predictions for the two relevant limits, i.e. high temperature and small chemical potential or high chemical potential and low temperature. This is clearly a serious drawback since those models cannot be fully tested. One of the few exceptions is the field correlator method [26], which is able to cover the full temperature-chemical potential-magnetic background field space and contains *ab initio* the property of confinement, which is expected to play a role, at variance with other models like, e.g., the Nambu-Jona-Lasinio model.

Indeed, the approach based on the FCM provides a systematic tool to treat nonperturbative effects in QCD by gauge invariant field correlators and gives a natural treatment of the dynamics of confinement (and of the deconfinement transition) in terms of the Gaussian, i.e., quadratic in the tensor $F_{\mu\nu}$ correlators for the chromoelectric (CE) field D^E and D_1^E and for the chromomagnetic field (CM) D^H and D_1^H. In particular, these correlators are related to the simplest nontrivial 2-point correlators for the CE and CM fields by

$$g^2\langle Tr_f[C_i(x)\Phi(x,y)C_k(y)\Phi(y,x)]\rangle = \delta_{ik}\left[D^C(z) + D_1^C(z) + z_4^2\frac{\partial D_1^C(z)}{\partial z^2}\right] \pm z_i z_k \frac{\partial D_1^C(z)}{\partial z^2}, \tag{13}$$

where $z = x - y$ and C indicates the CE (E) field or CM (H) field (the minus sign in the previous expression corresponds to the magnetic case) and

$$\Phi = P\exp\left[ig\int_x^y A^\mu dz_\mu\right] \tag{14}$$

is the parallel transporter.

The FCM has been extended to finite temperature and chemical potential [27–29], and the analytical results, in the Gaussian approximation, are in good agreement with the lattice data on thermodynamic quantities, (available for small μ_B only). Moreover, the application of the FCM for large values of the chemical potential allows us to obtain a simple expression of the equation of state of the quark-gluon matter in the range of the baryon density relevant for the study of neutron stars [34–37].

The comparisons with lattice data of the FCM predictions for the pressure (p/T^4), the interaction measure $\Delta/T^4 = (\epsilon - 3p)/T^4$, and the speed of sound at $\mu_B = 0$ and $\mu_B = 0.4$ GeV are depicted in Figs. 1, 2, and 3.

More recently, the effect of a background magnetic field B has been included in the FCM equation of state [30,31] and the quark (q) pressure and the gluon (g) pressure turn out to be

$$p_q(B) = \frac{N_c e_q B}{2\pi^2}\left[\phi(\mu) + \phi(-\mu) + \frac{2}{3}\frac{(\lambda(\mu)+\lambda(-\mu))}{e_q B} - \frac{e_q B}{24}(\tau(\mu)+\tau(-\mu))\right], \tag{15}$$

$$p_g = \frac{N_c^2 - 1}{3\pi^2}T^4\int_0^\infty \frac{z^3 dz}{\exp\left(z + \frac{9}{4}\frac{V_1(T)}{2T}\right) - 1}, \tag{16}$$

where $\phi(\mu)$, $\lambda(\mu)$, and $\tau(\mu)$ are, respectively, given by

$$\phi(\mu) = \int_0^\infty \frac{p_z dp_z}{1 + \exp(\frac{p_z - \bar{\mu}}{T})} \tag{17}$$

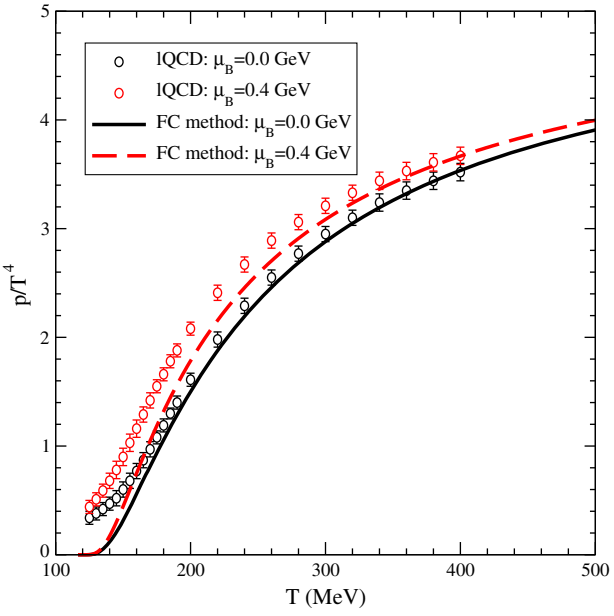

FIG. 1 (color online). Comparison with lattice data [2,4,38] of the pressure p evaluated by the FCM.

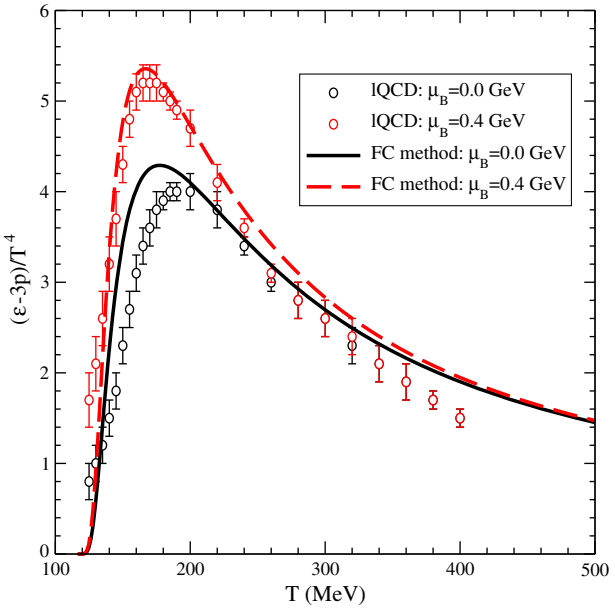

FIG. 2 (color online). Comparison with lattice data [2,4,38] of the interaction measure $\Delta = (\epsilon - 3p)/T^4$ evaluated by the FCM.

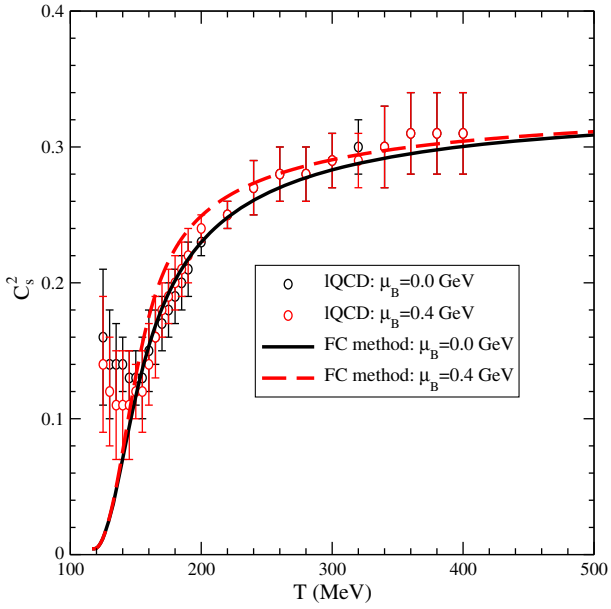

FIG. 3 (color online). Comparison with lattice data [2,4,38] of the speed of sound evaluated by the FCM.

$$\lambda(\mu) = \int_0^\infty \frac{p^4 dp}{\sqrt{p^2+\tilde{m}_q^2}} \frac{1}{\exp\left(\frac{\sqrt{p^2+\tilde{m}_q^2}-\bar{\mu}}{T}\right)+1}, \quad (18)$$

$$\tau(\mu) = \int_0^\infty \frac{dp_z}{\sqrt{p_z^2+\tilde{m}_q^2}} \frac{1}{\exp\left(\frac{\sqrt{p_z^2+\tilde{m}_q^2}-\bar{\mu}}{T}\right)+1}, \quad (19)$$

with $\bar{\mu} = \mu - \frac{V_1(T)}{2}$, $\tilde{m}_q^2 = m_q^2 + e_q B$, with m_q the current mass ($m_d = 5$ GeV, $m_u = 10$ MeV and $m_s = 140$ MeV) and

$$V_1(T) = c_0 + f(T/T_c) = 0.15 + 0.175\left(1.35\frac{T}{T_C} - 1\right)^{-1} \quad (20)$$

the quark-quark interaction potential.

In the limit $eB \to 0$ the only nonzero terms are $\lambda(\mu)$ and $\lambda(-\mu)$ and the previous formulas reproduce the case $\mu_B \neq 0$ [27].

In Fig. 4 one compares the ratio s/T^3 (s being the entropy density) evaluated in the FCM with lattice data for different values of the background field [38].

We consider a value of $eB = 0.6$ GeV^2 that corresponds to a maximum estimate of the magnetic field generated at the early times [39]. In some possible scenario a finite μ_B could also still be significant ($\mu_B \approx T$) at the QCD transition [14]. We consider $\mu_B = 0.4$ GeV, but we will see that its impact is quite limited.

The deconfinement temperature depends on μ_B and B and, therefore, the critical time t_c of the transition turns out to be 24, 21.5, 15.6, and 13.6 μs, respectively, for $\mu_B = 0.0$ GeV and $B = 0.0$, $\mu_B = 0.4$ GeV and $B = 0.0$, $\mu_B = 0.0$ and $B = 0.6$ GeV^2, and $\mu_B = 0.4$ GeV and $B = 0.6$ GeV^2.

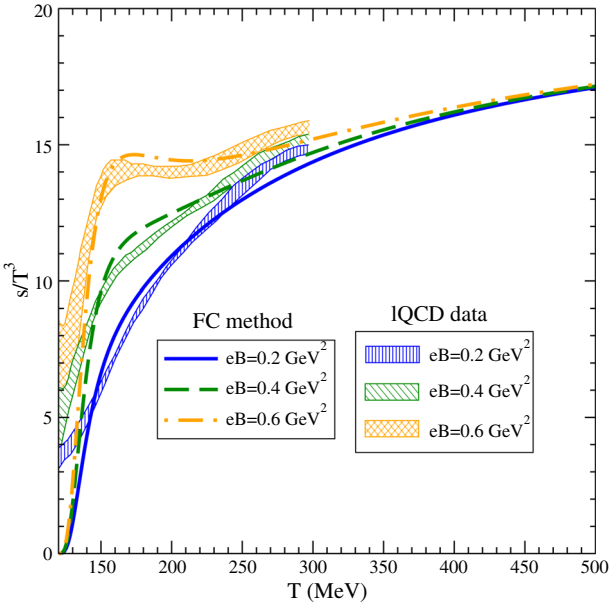

FIG. 4 (color online). Comparison of the FCM calculations for the entropy density with lattice data [12] for QCD in a background magnetic field B.

IV. FRIEDMANN EQUATION AND QUARK-GLUON PLASMA IN THE FCM

In the FCM the EoS of the quark-gluon plasma, i.e., $p(\epsilon)$, is obtained by direct calculations of $p(T)$ and $\epsilon(T)$, which inserted in the Friedman equation (8) give the time dependence of the temperature $T(t)$ and the corresponding time evolution of the thermodynamic quantities.

For the initial conditions $t_i = 1\mu s$, $T_i \simeq 500$ MeV, and $\epsilon_i \simeq 110$ GeV/fm^3, the function $T(t)$, the solution of the Friedman equation, is shown in Fig. 5 for different values of μ_B and compared with the MIT bag model with the same initial conditions and a bag pressure $B_{\rm mit} = 220$ MeV/fm^3.

The arrows in Fig. 5 (and in the next figures) correspond to the critical temperatures for the different specific sets of parameters and, therefore, to the corresponding critical time t_c when the phase transition occurs. The critical temperature $T_c = 160$ MeV for $\mu_B = 0$ corresponds to $t_c \simeq 25$ μs, which decreases to $t_c \simeq 22$ μs for $\mu_B = 0.4$ GeV. The curves are also plotted for $t > t_c$, i.e., for temperature below the transition point, although the effective degrees of freedom below T_c are not included in the present paper.

The equation of state p/ϵ in the FCM, reported in Fig. 6, shows a small dependence on μ_B up to 400 MeV.

The role of the background magnetic field in the calculation of $T(t)$ and in the time evolution of the EoS are reported in Fig. 7 and in Fig. 8, which also describe the combined effect of the finite density and the background magnetic field.

Notice that the results in the MIT bag model (green curves in Figs. 6, 7, and 8) are clearly different from the EoS evaluated by the FCM and that the magnetic field B can move down t_c by nearly a factor of 2.

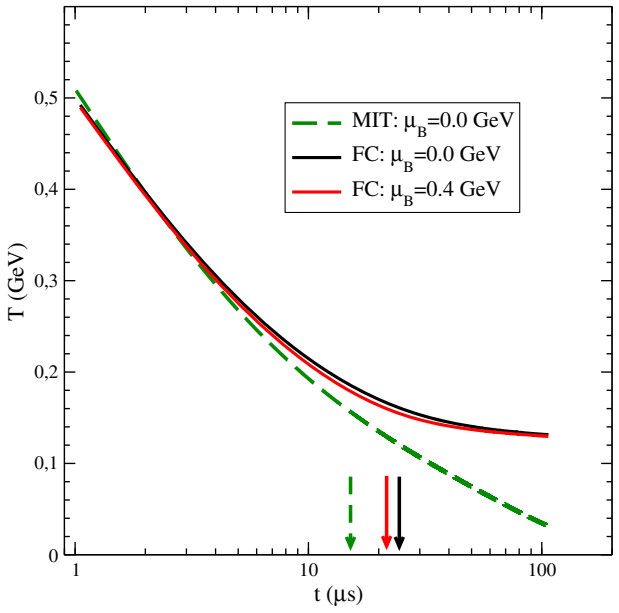

FIG. 5 (color online). $T(t)$ solution of the Friedmannn equation (8) by using the EoS in the FCM. The arrows indicate the critical time, t_c of the transition given in the text.

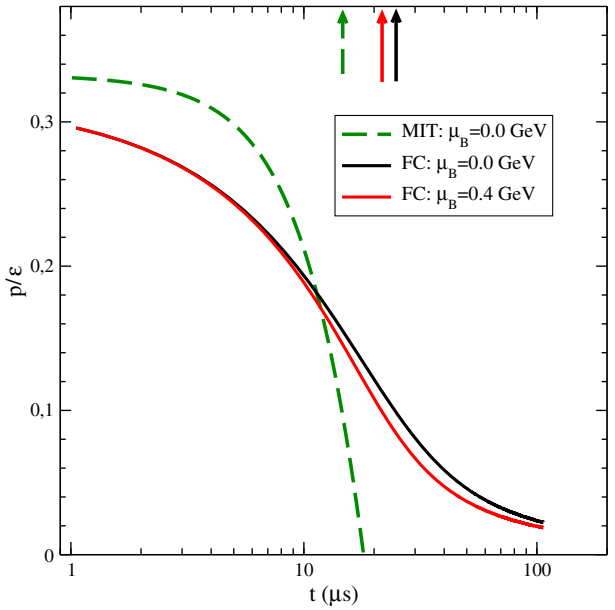

FIG. 6 (color online). EoS in the FCM for finite chemical potential. The green curve refers to the MIT bag model calculation with the parameters given in the text.

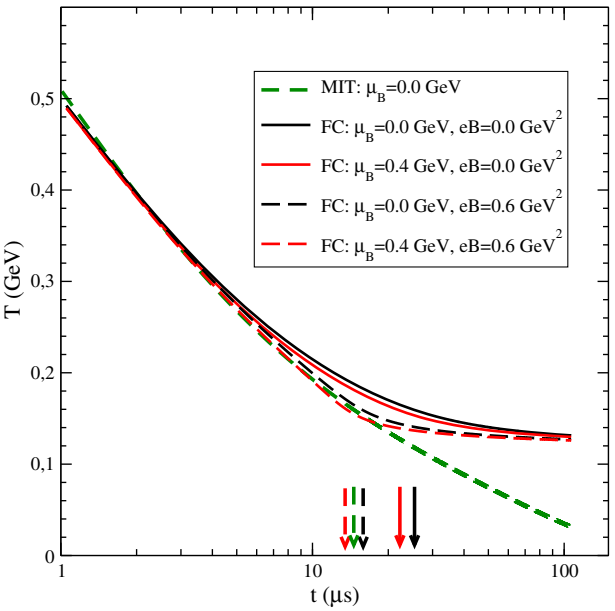

FIG. 7 (color online). The temperature profile $T(t)$ for different values of μ_B and B.

V. ELECTROWEAK CONTRIBUTION TO THE EQUATION OF STATE

The time evolution of the cosmological parameters depend on the EoS of the entire system and, therefore,

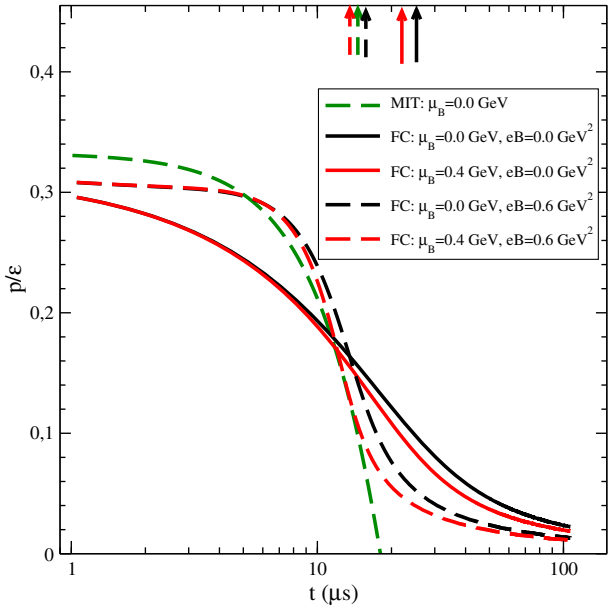

FIG. 8 (color online). Time evolution of the EoS in the FCM for finite chemical potential and background magnetic field.

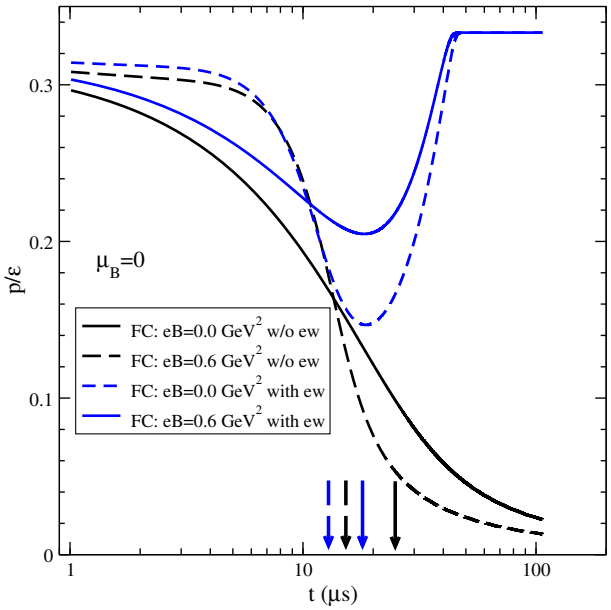

FIG. 10 (color online). EoS with and without the electroweak contribution and the background magnetic field for $\mu_B = 0$.

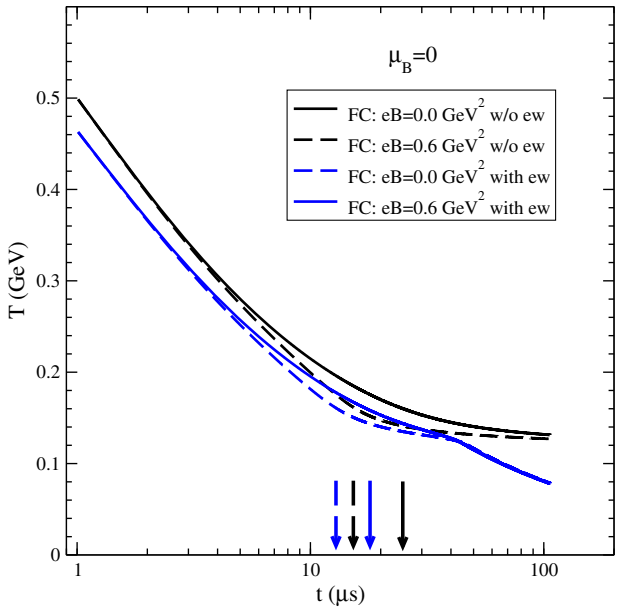

FIG. 9 (color online). $T(t)$ with and without the electroweak contribution and the background magnetic field.

one has to take into account not only the quark gluon plasma degrees of freedom, discussed in the previous section, but also the contributions of the electroweak sector to the pressure p_{ew} and the energy density ϵ_{ew}. The total pressure and energy density are, therefore, $p_{\rm tot} = p_{qgp} + p_{ew}$ and $\epsilon_{\rm tot} = \epsilon_{qgp} + \epsilon_{ew}$.

The electroweak sector is described as a system of free massless particles, i.e.,

$$\epsilon_{ew} = g_{ew}\frac{\pi^2}{30}T^4, \tag{21}$$

$$p_{ew} = g_{ew}\frac{\pi^2}{90}T^4, \tag{22}$$

with the number of degrees of freedom $g_{ew} = 14.45$.

The temperature profile is almost unmodified by the introduction of the electroweak contributions as one can see from Fig. 9, where the curves are plotted for $\mu_B = 0$, since the chemical potential produces negligible changes (see Figs. 5 and 6).

On the other hand, the EoS of the entire system strongly reflects the presence of the electroweak terms. In Fig. 10 the time evolution of p/ϵ for the entire system is depicted and, indeed, one immediately notes that in the time interval $t \simeq 10$–25 μs, the electroweak part has a minor role, but near the critical temperature there is a clear change in the shape and the EoS tends to $p = \epsilon/3$, i.e., to a radiation-dominated universe, for the long time. The curves are plotted for time longer than t_c, just to show the behavior below T_c without the contribution of the colorless effective degrees of freedom after the transition, which is not included in the present analysis and will be discussed in a forthcoming paper.

VI. EVOLUTION OF THE COSMOLOGICAL PARAMETERS

The evolution of the cosmological parameters during the deconfinement transition is directly related to the EoS. In Figures 11 and 12, respectively, depict the time behavior of the scale factor and of $H(t)$ for different values of the

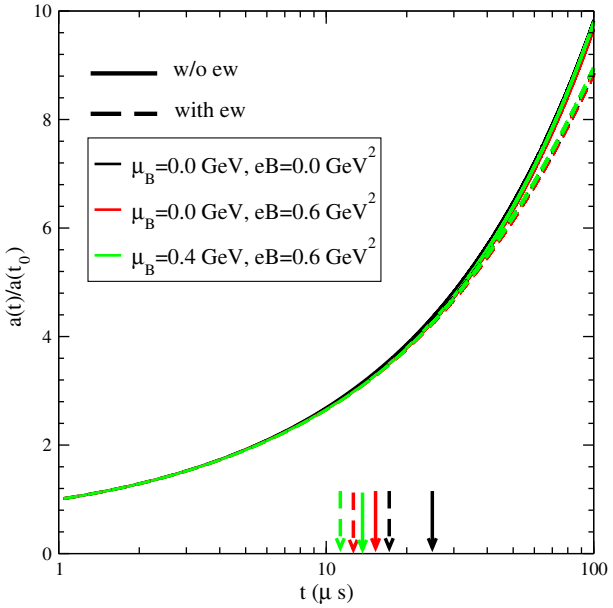

FIG. 11 (color online). Time evolution of the scale factor for finite chemical potential, with and without the electroweak contribution and the background magnetic field.

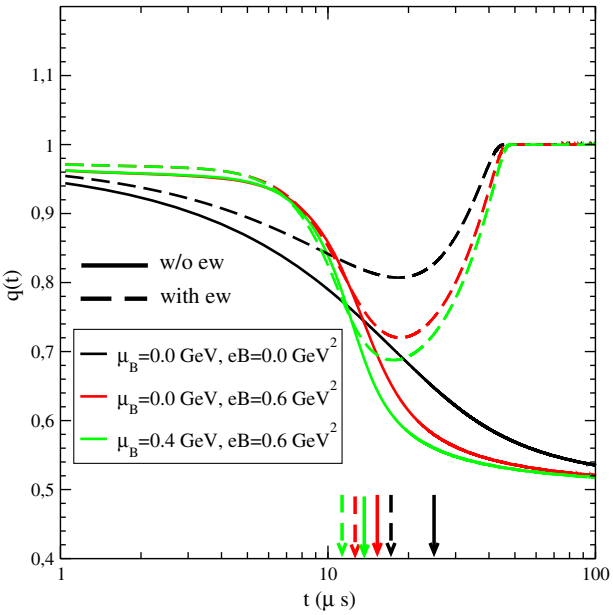

FIG. 13 (color online). $q(t)$ for finite chemical potential, with and without the electroweak contribution and the background magnetic field.

chemical potential and the magnetic field with and without the electroweak contribution. The final result is essentially independent of the specific setting.

However, the deceleration $q(t)$ and the jerk $j(t)$ strongly follow the time evolution of the EoS (in Fig. 10). Both q and j (see Fig. 13 and Fig. 14), after initial values corresponding to a radiation-dominated universe ($q \simeq 1$, $j \simeq 3$), tend to $q \simeq 1/2$ and $j \simeq 1$, typical of a matter-dominated universe, approaching from above the critical temperature. Indeed, without the electroweak sector, the values of the cosmological parameters for time $t \simeq 100\ \mu$s would be the typical ones of a matter-dominated universe. However, near the transition point, the electroweak terms in the EoS start to be relevant and, therefore, $q \to 1$ and $j \to 3$ for the long time.

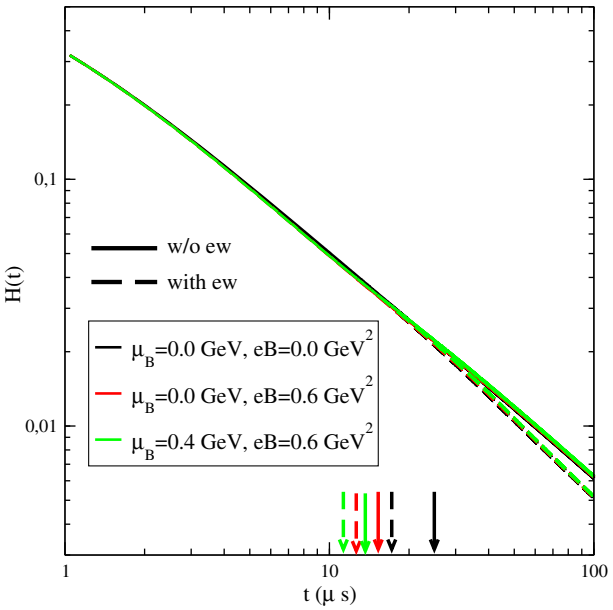

FIG. 12 (color online). $H(t)$ for finite chemical potential, with and without the electroweak contribution and the background magnetic field.

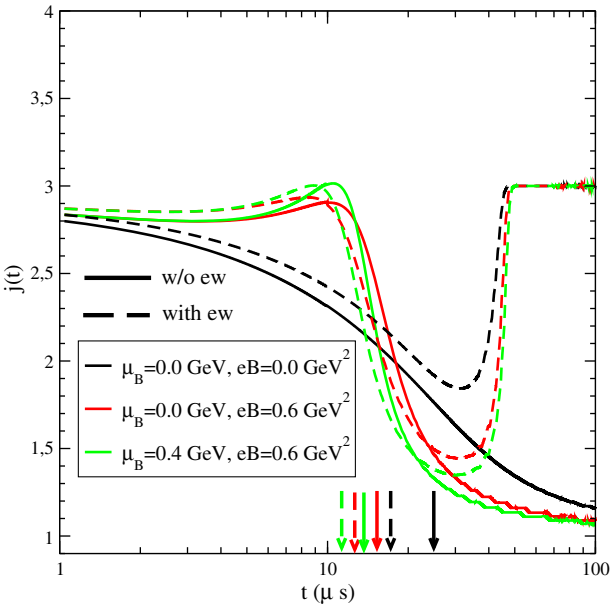

FIG. 14 (color online). $j(t)$ for finite chemical potential, with and without the electroweak contribution and the background magnetic field.

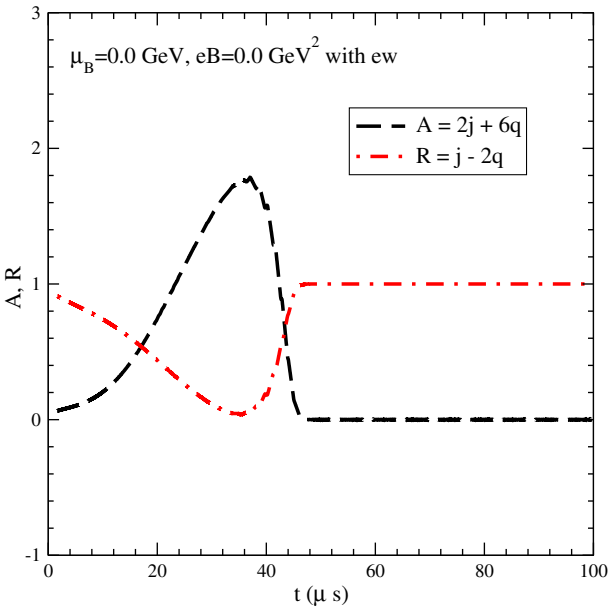

FIG. 15 (color online). Time evolution of A and R according to the simple model in Eq. (5) but using $q(t)$ and $j(t)$ in the FCM.

A possible interpretation of this peculiar behavior can be made with the help of the simple model in Sec. I, where $A = -2j + 6q$ and $R = j - 2q$ are, respectively, the matter and radiation terms in the Friedmann equation. For a matter-dominated flat universe, $A = 1$ and $R = 0$; for a radiation-dominated one, $A = 0$ and $R = 1$. Since in Eq. (5) there is no interaction between the two components, $A + R = 1$. Of course, this condition is not satisfied by using q and j calculated in the FCM, and different values of A and R signal a mixture and/or an interaction between the two components.

By using the values of q and j in the FCM, the time evolution of A and R is given in Fig. 15. R decreases from an initial value $\simeq 1$ to $\simeq 0.3$ at $t \simeq 25$ μs and to $\simeq 0$ at $t \simeq 32$ μs and then quickly reaches again the value of a radiation-dominated universe. A has the corresponding evolution, starting from $A \simeq 0.0$, increasing to a value $\simeq 1$ at $t \simeq 25$ μs, with a maximum $A \simeq 1.8$ at $t \simeq 35$ μs, and finally decreasing to $A \simeq 0$, i.e., a radiation-dominated universe. Therefore, there is a clear mixture of the two components which strongly interact with each other.

The observed behavior of A and R implies that above the transition and before the dominance of the electroweak sector, the system has essentially the EoS of interacting matter. On the other hand, above T_c the color degrees of freedom are still not neutralized and, therefore, the previous results suggest the formation of colored and massive clusters near the deconfinement transition before the formation of colorless bound states.

Indeed, this is a well-known interpretation of the QCD EoS at finite temperature in terms of quasiparticles where quasiquarks and quasigluons have dynamical, temperature-dependent, effective masses which mimic the interaction and that near T_c are large, i.e., in the range $\simeq 0.6$–1.2 GeV $\mu_B = 0 = B$ [40–43].

VII. COMMENTS AND CONCLUSIONS

The analysis in the previous sections shows that during the deconfinement transition, the time evolution of the scale factor and of $H(t)$ are weakly sensitive to the EoS and that, on the contrary, the cosmological parameters $q(t)$ and $j(t)$ follow the behavior of the ratio p/ϵ. Starting from a radiation-dominated universe, the time evolution of the EoS indicates that above and near the transition time t_c the entire system (quark gluon plasma + electroweak sector) is in a matter-dominated state ($q \approx 0.5$ and $j \approx 1$). For a longer time, the evolution is again dominated by the radiation EoS. The introduction of a finite baryon chemical potential and a background magnetic field do not qualitatively change this dynamical picture.

On the other hand, since above and near T_c one has color degrees of freedom, the matter state which drives the EoS is, presumably, formed by color massive objects, as suggested by the quasiparticle models [40,41,44]. Indeed, the behavior of $A(t)$, i.e., of the matter content of the system, reported in Fig. 15 is analogous to the time evolution of the interaction measure $(\epsilon - 3p)/T^4$, in Fig. 16, where the electroweak sector has no role.

It should be stressed that although the QCD lattice data have been described by the FCM, the final results are independent of this specific framework and depend on the nonperturbative QCD EoS only.

Below T_c, i.e. for $t > t_c$, the effective degrees of freedom can be described by a hadron resonance gas (HRG) model

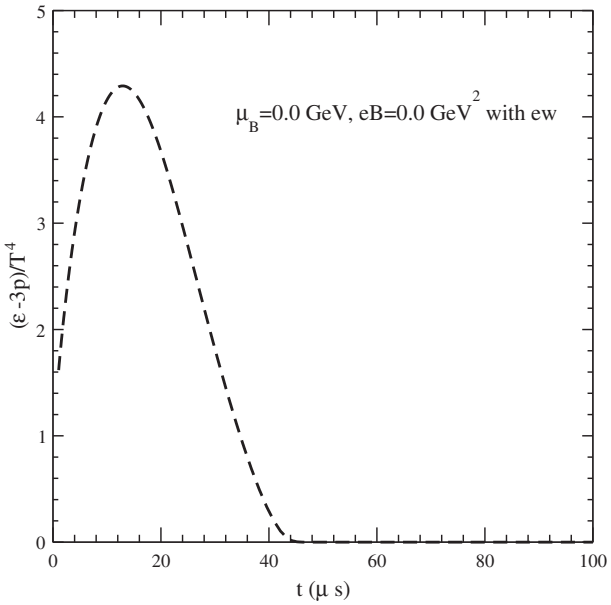

FIG. 16. Time evolution of the interaction measure.

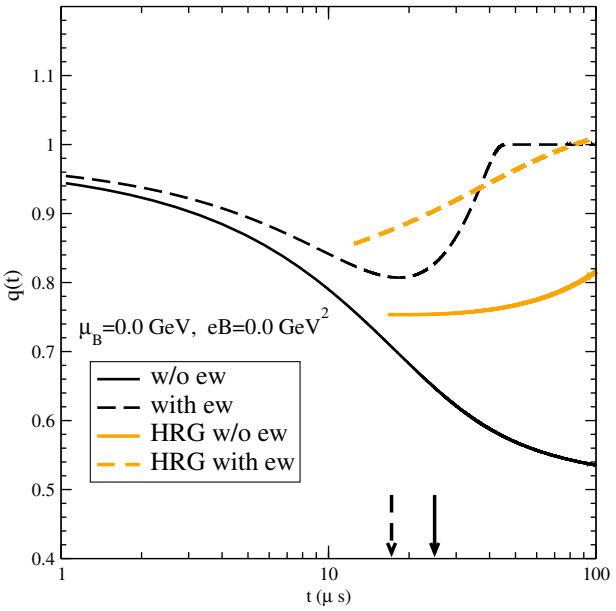

FIG. 17 (color online). Time evolution of q (yellow line) below T_c where the hadronic sector is described by the HRG without excluded volume [46].

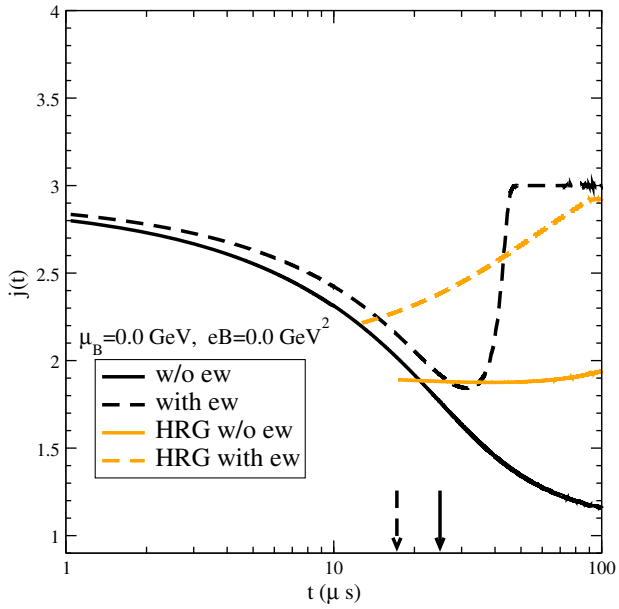

FIG. 18 (color online). Time evolution of j (yellow line) below T_c where the hadronic sector is described by the HRG without excluded volume [46].

which is able to give a good description of the QCD matter down to $T \sim 1/3T_c$ [45,46].

The HRG contribution, in the formulation in Ref. [46], to the EoS has been included in the Friedmann equations in such a way that one can consistently follow the time evolution of the cosmological parameters down to $t \approx 100$ fm/c. The final results are depicted in Figs. 17 and 18 where the yellow lines show the behavior of q and j when the system contains the HRG and the electroweak sector.

ACKNOWLEDGMENTS

V. Greco and S. Plumari acknowledge the support of the ERC-StG Grant under the QGPDyn project.

[1] Y. Aoki, G. Endrodi, Z. Fodor, S. D. Katz, and K. K. Szabo, Nature (London) **443**, 675 (2006).
[2] S. Borsanyi, Z. Fodor, C. Hoelbling, S. D. Katz, S. Krieg, and K. K. Szabó, Phys. Lett. B **730**, 99 (2014).
[3] A. Bazavov *et al.*, Phys. Rev. D **85**, 054503 (2012).
[4] A. Bazavov *et al.*, Phys. Rev. D **90**, 094503 (2014).
[5] M. Asakawa and K. Yazaki, Nucl. Phys. **A504**, 668 (1989).
[6] M. A. Stephanov, *Proc. Sci.*, LAT2006 (2006) 024.
[7] S. Roessner, C. Ratti, and W. Weise, Phys. Rev. D **75**, 034007 (2007).
[8] G. Y. Shao, M. Di Toro, V. Greco, M. Colonna, S. Plumari, B. Liu, and Y. X. Liu, Phys. Rev. D **84**, 034028 (2011).
[9] M. Chojnacki and W. Florkowski, Acta Phys. Pol. B **38**, 3249 (2007).
[10] W. Broniowski, M. Chojnacki, W. Florkowski, and A. Kisiel, Phys. Rev. Lett. **101**, 022301 (2008).
[11] C. Bonati, M. D'Elia, M. Mariti, F. Negro, and F. Sanfilippo, Phys. Rev. D **89**, 054506 (2014).
[12] G. S. Bali, F. Bruckmann, G. Endrodi, S. D. Katz, and A. Schfer, J. High Energy Phys. 08 (2014) 177.
[13] T. Boeckel, S. Schettler, and J. Schaffner-Bielich, Prog. Part. Nucl. Phys. **66**, 266 (2011).
[14] T. Boeckel and J. Schaffner-Bielich, Phys. Rev. D **85**, 103506 (2012).
[15] A. Tawfik and T. Harko, Phys. Rev. D **85**, 084032 (2012).
[16] A. Tawfik, M. Wahba, H. Mansour, and T. Harko, Ann. Phys. (Berlin) **523**, 194 (2011).
[17] C. Schmid, D. J. Schwarz, and P. Widerin, Phys. Rev. D **59**, 043517 (1999);
[18] G. L. Guardo, V. Greco, and M. Ruggieri, AIP Conf. Proc. **1595**, 224 (2014).
[19] W. Florkowski, Nucl. Phys. **A853**, 173 (2011).
[20] S. M. Sanches, F. S. Navarra, and D. A. Fogaa, Nucl. Phys. **A937**, 1 (2015).
[21] V. R. C. Mouro Roque and G. Lugones, Phys. Rev. D **87**, 083516 (2013).

[22] D. J. Schwarz and M. Stuke, J. Cosmol. Astropart. Phys. 11 (2009) 025; 10 (2010) E01.
[23] D. Boyanovsky, H. J. de Vega, and D. J. Schwarz, Annu. Rev. Nucl. Part. Sci. **56**, 441 (2006);
[24] D. J. Schwarz, Nucl. Phys. **A642**, c336 (1998).
[25] T. Kalaydzhyan and E. Shuryak, Phys. Rev. D **91**, 083502 (2015).
[26] For a review of the FCM, see A. Di Giacomo, H. G. Dosch, V. I. Shevchenko, and Y. A. Simonov, Phys. Rep. **372**, 319 (2002).
[27] Yu. A. Simonov and M. A. Trusov, JETP Lett. **85**, 598 (2007).
[28] Yu. A. Simonov and M. A. Trusov, Phys. Lett. B **650**, 36 (2007).
[29] E. V. Komarov and Y. A. Simonov, Ann. Phys. (Amsterdam) **323**, 1230 (2008).
[30] V. Orlovsky and Y. A. Simonov, Phys. Rev. D **89**, 054012 (2014).
[31] V. Orlovsky and Y. A. Simonov, Phys. Rev. D **89**, 074034 (2014).
[32] M. Dunajski and G. Gibbons, Classical Quantum Gravity **25**, 235012 (2008).
[33] Yu. L. Bolotin *et al.*, arXiv:1502.00811.
[34] M. Baldo, G. F. Burgio, P. Castorina, S. Plumari, and D. Zappal, Phys. Rev. D **78**, 063009 (2008).
[35] G. F. Burgio, M. Baldo, P. Castorina, S. Plumari, and D. Zappal, *Proc. Sci.*, CONFINEMENT8 (2008) 149.
[36] M. G. Alford, G. F. Burgio, S. Han, G. Taranto, and D. Zappalá, arXiv:1501.07902.
[37] S. Plumari, G. F. Burgio, V. Greco, and D. Zappala, Phys. Rev. D **88**, 083005 (2013).
[38] Sz. Borsányi, G. Endrődi, Z. Fodor, S. D. Katz, S. Krieg, C. Ratti, and K. K. Szabó, J. High Energy Phys. 08 (2012) 053.
[39] T. Vachaspati, Phys. Lett. B **265**, 258 (1991).
[40] P. Castorina, D. E. Miller, and H. Satz, Eur. Phys. J. C **71**, 1673 (2011).
[41] S. Plumari, W. M. Alberico, V. Greco, and C. Ratti, Phys. Rev. D **84**, 094004 (2011).
[42] L. Oliva, P. Castorina, V. Greco, and M. Ruggieri, Phys. Rev. D **88**, 097502 (2013).
[43] P. Castorina and M. Mannarelli, Phys. Rev. C **75**, 054901 (2007).
[44] M. Ruggieri, P. Alba, P. Castorina, S. Plumari, C. Ratti, and V. Greco, Phys. Rev. D **86**, 054007 (2012).
[45] C. Ratti, S. Borsányi, Z. Fodor, C. Hoelbling, S. D. Katz, S. Krieg, and K. K. Szabó (Wuppertal-Budapest Collaboration), Nucl. Phys. **A855**, 253 (2011).
[46] V. Vovchenko, D. V. Anchishkin, and M. I. Gorenstein, Phys. Rev. C **91** 2, 024905 (2015).